J Neurophysiol 120: 372–384, 2018.
First published April 18, 2018; doi:10.1152/jn.00887.2017.

RESEARCH ARTICLE | *Higher Neural Functions and Behavior*

Neural mechanisms of speed-accuracy tradeoff of visual search: saccade vigor, the origin of targeting errors, and comparison of the superior colliculus and frontal eye field

Thomas R. Reppert, Mathieu Servant, Richard P. Heitz, and Jeffrey D. Schall
Center for Integrative and Cognitive Neuroscience, Vanderbilt Vision Research Center, Department of Psychology, Vanderbilt University, Nashville, Tennessee

Submitted 13 December 2017; accepted in final form 17 April 2018

Reppert TR, Servant M, Heitz RP, Schall JD. Neural mechanisms of speed-accuracy tradeoff of visual search: saccade vigor, the origin of targeting errors, and comparison of superior colliculus and frontal eye field. *J Neurophysiol* 120: 372–384, 2018. First published April 18, 2018; doi:10.1152/jn.00887.2017.—Balancing the speed-accuracy tradeoff (SAT) is necessary for successful behavior. Using a visual search task with interleaved cues emphasizing speed or accuracy, we recently reported diverse contributions of frontal eye field (FEF) neurons instantiating salience evidence and response preparation. Here, we report replication of visual search SAT performance in two macaque monkeys, new information about variation of saccade dynamics with SAT, extension of the neurophysiological investigation to describe processes in the superior colliculus (SC), and a description of the origin of search errors in this task. Saccade vigor varied idiosyncratically across SAT conditions and monkeys but tended to decrease with response time. As observed in the FEF, speed-accuracy tradeoff was accomplished through several distinct adjustments in the superior colliculus. In "Accurate" relative to "Fast" trials, visually responsive neurons in SC as in FEF had lower baseline firing rates and later target selection. The magnitude of these adjustments in SC was indistinguishable from that in FEF. Search errors occurred when visual salience neurons in the FEF and the SC treated distractors as targets, even in the Accurate condition. Unlike FEF, the magnitude of visual responses in the SC did not vary across SAT conditions. Also unlike FEF, the activity of SC movement neurons when saccades were initiated was equivalent in Fast and Accurate trials. Saccade-related neural activity in SC, but not FEF, varied with saccade peak velocity. These results extend our understanding of the cortical and subcortical contributions to SAT.

NEW & NOTEWORTHY Neurophysiological mechanisms of speed-accuracy tradeoff (SAT) have only recently been investigated. This article reports the first replication of SAT performance in nonhuman primates, the first report of variation of saccade dynamics with SAT, the first description of superior colliculus contributions to SAT, and the first description of the origin of errors during SAT. These results inform and constrain new models of distributed decision making.

decision making; speed-accuracy tradeoff; stochastic accumulator models; superior colliculus; vigor

INTRODUCTION

The speed-accuracy tradeoff (SAT) is a fundamental behavioral phenomenon (Heitz, 2014). Computational decision models explain SAT in terms of a stochastic accumulation of noisy sensory evidence from a baseline level over time; responses are produced when the accumulated evidence for one choice reaches a threshold. Slower, more accurate responses are achieved by elevating the threshold; faster, less accurate responses are produced by lowering the threshold. Many laboratories have provided evidence linking the stochastic accumulation process with the activity of specific neurons in the frontal eye field (FEF) (Boucher et al. 2007; Ding and Gold 2012; Hanes and Schall 1996; Kim and Shadlen 1999; Purcell et al. 2010, 2012; Woodman et al. 2008), lateral intraparietal area (LIP) (Roitman and Shadlen 2002; Wong et al. 2007; but see Latimer et al. 2015; Yates et al. 2017), motor and premotor cortex (Thura et al. 2012), superior colliculus (SC) (Ratcliff et al. 2003, 2007), and basal ganglia (Ding and Gold 2010). However, neurophysiological studies investigating SAT have only recently appeared (Hanks et al. 2014; Heitz and Schall 2012; Thura and Cisek 2016, 2017), and all have focused on forebrain structures. We now replicate major findings in two more monkeys and show that subcortical processes in the superior colliculus also contribute to SAT for saccades during visual search. We also show how search errors arise in this task and report new findings about idiosyncratic and systematic variation of saccade dynamics across SAT conditions.

METHODS

All procedures were approved by the Vanderbilt Institutional Animal Care and Use Committee in accordance with the United States Department of Agriculture and Public Health Service Policy on Humane Care and Use of Laboratory Animals.

Task. Four bonnet macaques (*Macaca radiata*), identified as Q, S, Da, and Eu, performed a form visual search task for a target item (a T or L shape randomly oriented) presented among seven distractor items (consisting of L or T shapes randomly oriented) (Fig. 1). Trials began when monkeys fixated a central cue for ~1 s. Each monkey was extensively trained to associate the color of the fixation cue (red or green) with a task condition ("Accurate" or "Fast"). After fixation, an iso-eccentric array of T/L shapes appeared, of which one was the target item for that day. Distractor items were drawn randomly from the nontarget set and oriented randomly in the cardinal positions.

Address for reprint requests and other correspondence: J. D. Schall, Dept. of Psychology, Vanderbilt Univ., PMB 407817, 2301 Vanderbilt Place, Nashville, TN 37240-7817 (e-mail: jeffrey.d.schall@vanderbilt.edu).

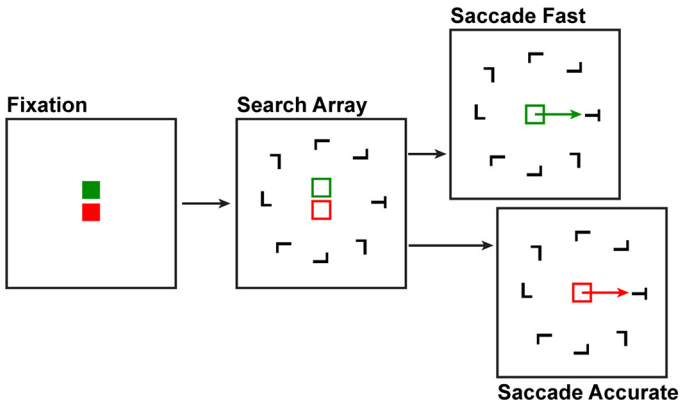

Fig. 1. Visual search paradigm with speed-accuracy tradeoff. Trials began with a fixation cue signifying whether the trial was to be Fast (green) or Accurate (red). After a fixation period of ~1 s, an isoeccentric array of 8 T/L shapes appeared, of which one was the target for that session. Monkeys searched for the target item (rotated T or L) presented with seven distractors (rotated L or T). In the Fast and Accurate conditions, correct responses were only rewarded when executed before and after an unsignaled deadline, respectively. In some sessions, distractors were of homogeneous orientation; in other sessions, they were randomly rotated. Fixation point, search shapes, and viewing screen are not drawn to scale.

Sessions comprised miniblocks of 10–20 trials of a single SAT condition. In the Accurate condition, saccades to the target item were rewarded if response time (RT) exceeded an unsignaled deadline. Unless otherwise specified, we use RT to refer to response time relative to array stimulus appearance. The deadline was adjusted to optimize the yield of useful data against sustained performance. In this data set, the deadline for successful trials in the Accurate condition was set to 500 ms (Q), 427 ± 5 ms (S), 435 ± 7 ms (Da), and 445 ± 6 ms (Eu) (means ± SE across sessions), respectively. In the Accurate condition, responses with incorrect timing and/or direction were followed by a 4-s time-out. In the Fast condition, saccades to the target item were rewarded only if the saccade to the target occurred before an unsignaled deadline. In this data set, the deadline for successful trials in the Fast condition was 370 ± 10 ms (Q), 386 ± 7 ms (S), 365 ± 14 ms (Da), and 429 ± 21 ms (Eu) (means ± SE), respectively. Saccades executed after the deadline in the Fast condition were followed by a 4-s time-out. However, inaccurate saccades made before the deadline in the Fast condition (i.e., with correct timing) had no time-out. The lack of time-out following misdirected saccades was used to incentivize quick responses. We divided the visual space into eight octants (± 22.5° of target). Responses were deemed accurate when the saccade end point was within the octant specified by the target.

Neural data acquisition. Details of the methods have been reported previously (Heitz and Schall 2012). Briefly, neural spikes were sampled in the SC and FEF using tungsten microelectrodes (2–4 MΩ; FHC, Bowdoin, ME). Location was verified by evoking eye movements with <50 μA electrical microstimulation. The number of electrodes lowered during a given session ranged from 1 to 9. Single-unit waveforms were digitized and sorted offline (Offline Sorter; Plexon, Dallas, TX).

Neural data analysis. Spike trains were convolved with a kernel that resembled a postsynaptic potential to create a spike density function (SDF) (τ_{growth} = 1 ms, τ_{decay} = 20 ms; Thompson et al. 1996). For visually responsive activity, SDFs were normalized to the peak average activity during the 1-s time interval poststimulus appearance. For saccade-related activity, SDFs were normalized to the peak average activity in the time interval 100 ms presaccade to 100 ms postsaccade initiation. Normalization factors were computed across all conditions and behavioral outcomes (i.e., over all SAT conditions, all RTs, and correct and errant responses) in a particular session.

Neurons were categorized into three major types based on gross function: visual, visuo-movement, and movement. Although classification operates along a continuum, many observations demonstrate that these populations are functionally distinct (Cohen et al. 2009; Gregoriou et al. 2012; Ray et al. 2009). Visual neurons increase discharge rates significantly immediately following search array presentation but have little or no saccade-related modulation. Movement neurons increase discharge rate significantly before saccade initiation but have little or no visual response. Visuo-movement neurons exhibit both periods of modulation. To classify neurons, we analyzed single-unit activity from a memory-guided saccade task. The primary function of this task was to dissociate visual activity related to stimulus appearance from movement activity related to saccade execution. To test for visual responses, we used Student's *t*-tests to compare the average activity in the interval 75–100 ms after target presentation to the activity in the 100-ms interval preceding target presentation. To test for presaccadic activity, we used Student's *t*-tests to compare the average activity in the 100-ms interval before saccade initiation to the activity in the interval 500–400 ms before saccade initiation.

Behavioral analyses. All gaze data were collected with video-oculography (Eyelink, SR Research) at a sampling rate of 1,000 Hz. The data were filtered with a 3rd-order Butterworth low-pass filter with a cutoff frequency of 80 Hz. The data were then differentiated to velocity traces, and a cutoff velocity of 20°/s was used to identify all saccades. Because of the limited size of the visual field of the video-oculography, final gaze position of the response was lost on a fraction of trials. That is, on these trials, response time was still available, but saccade displacement and vigor were not. The fraction of trials with inaccurate gaze end points was 11.7% (Da), 8.7% (Eu), 9.8% (Q), and 19.2% (S). Moreover, any eye movements that did not meet the following criteria were removed from all analyses: *1*) duration between 10 and 80 ms, *2*) peak velocity between 200 and 1,000°/s, *3*) displacement greater than 2.5°, and *4*) initial radial position less than 2.0° from the fixation point. For each trial, we labeled the first saccade satisfying these characteristics as the task-relevant saccade for that trial. The fraction of trials without a task-relevant response was 14.9% (Da), 5.5% (Eu), 14.0% (Q), and 12.4% (S).

Saccade vigor. To characterize saccade vigor, we quantified the relationship between displacement and peak velocity of all task-relevant saccades. This relationship is typically linear for saccades of displacement up to ~20° (Bahill et al. 1975; Collewijn et al. 1988). The majority of saccades recorded from all monkeys shifted gaze less than 9°. Therefore, we fitted the relationship between displacement and peak velocity to a linear function constrained to pass through the origin: $g(x) = \alpha \cdot x$. Given the average main sequence relationship, we then computed the vigor of saccade j with displacement x as the ratio between the measured velocity and the expected velocity $v_j(x)/\hat{v}_j(x)$. Ratios > 1.0 measure saccades with greater vigor than the saccade population average. We used this measure of vigor to quantify changes in saccade dynamics across SAT conditions and response times.

Statistical analyses. We used paired *t*-tests to compare neural activity in Fast and Accurate conditions. We used unpaired *t*-tests to compare neural activity in the SC and FEF. Corresponding *t*-statistics and *P* values are provided. We used JZS Bayes Factor (BF; r = 0.707) to assess strength of findings of invariance in the behavioral and neural data (Rouder et al. 2009, 2012). We used repeated-measures ANOVA (RM-ANOVA) to test the interaction between RT and error rate, and RT and saccade vigor. To determine when neurons responded differently to two SAT conditions, or when the target as compared with distractors appeared in the receptive field (RF) or movement field (MF), we used a ms-by-ms one-sided Mann-Whitney *U*-test. Target selection time (TST) was the first successive 30 ms with a significant difference at $P < 0.01$.

RESULTS

Response time and accuracy. An analysis of the performance of Q and S was previously published (Heitz and Schall 2012). Performance measures of Da and Eu were collected during 16 sessions (Da: 9 sessions; Eu: 7). Monkeys Da and Eu adjusted RT in accordance with task condition in each session. Average RT across sessions during Fast condition was 280 ± 9 ms (Da) and 354 ± 13 ms (Eu) (means ± SE; Fig. 2*A*). Average RT during Accurate condition was 498 ± 9 ms (Da) and 510 ± 17 (Eu). Response time adjustments were immediate upon receiving a new SAT condition cue (Fig. 2*B*), replicating the performance of monkeys Q and S.

The Accurate and Fast conditions used response deadlines similar to some human studies (Heitz and Engle 2007; Rinkenauer et al. 2004). These deadlines were adjusted so that ~70–80% of saccades were executed with the correct timing. Figure 2*C* presents RT distributions relative to the deadlines for all four monkeys. The prior report of performance data from Q and S did not include this measure, but these distributions support future computational modeling.

In addition to timing errors, we also analyzed saccade end-point errors (i.e., gaze shifts to a nontarget item). Average

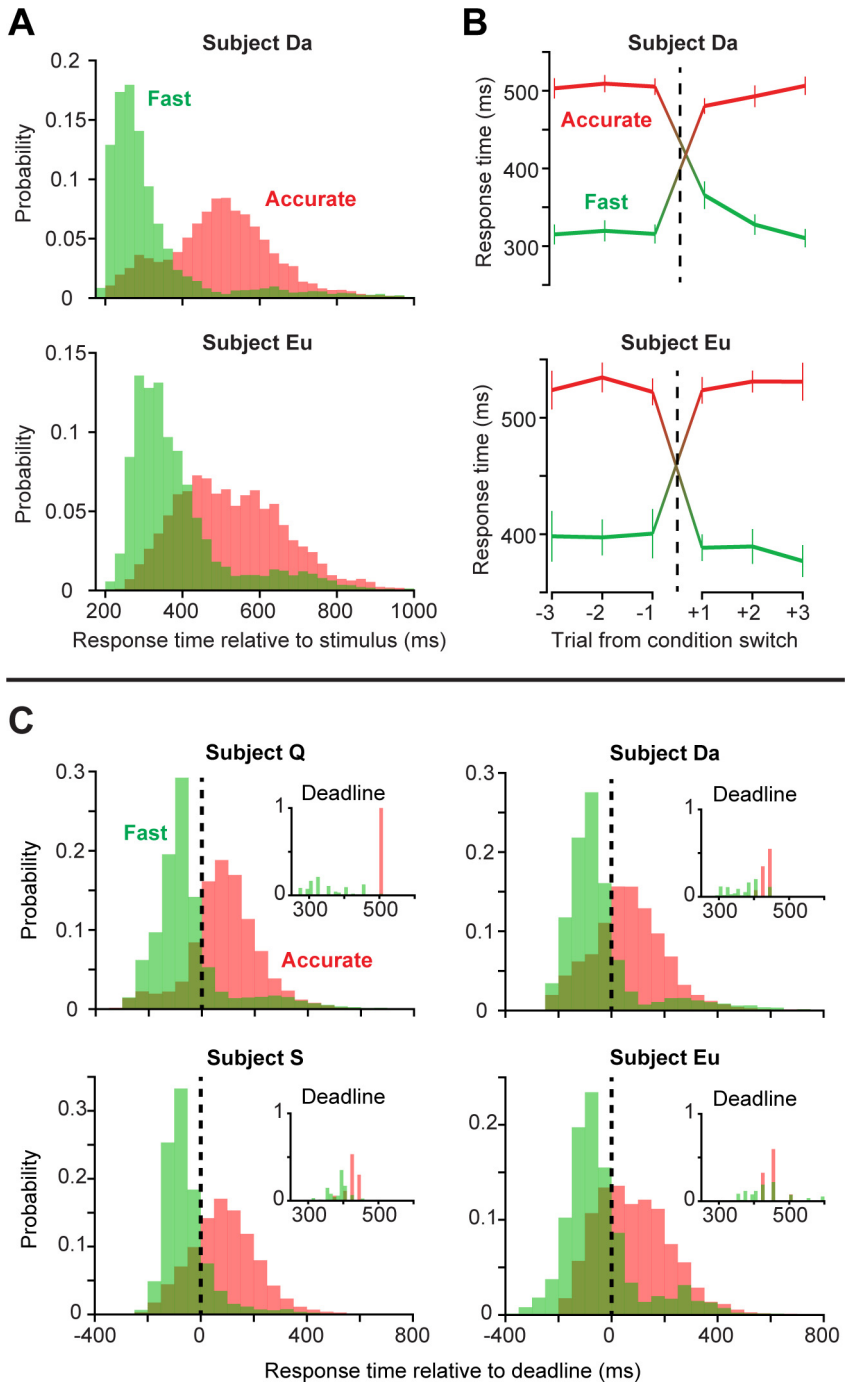

Fig. 2. Response time adjustments during speed-accuracy tradeoff. *A*: probability distributions of RT on Fast (green) and Accurate (red) trials for monkeys Da and Eu. Distributions include trials pooled across all recording sessions for each monkey. *B*: change in RT on three trials immediately preceding and following a switch in task condition. Both monkeys altered RT on the trial immediately following a change in fixation cue color, signaling condition switch. Error bars show means ± SE. *C*: probability distributions of RT relative to response deadline for all four monkeys. *Insets*: probability distributions of response deadline. All responses that occurred after the deadline in the Fast condition or before the deadline in the Accurate condition were considered timing errors.

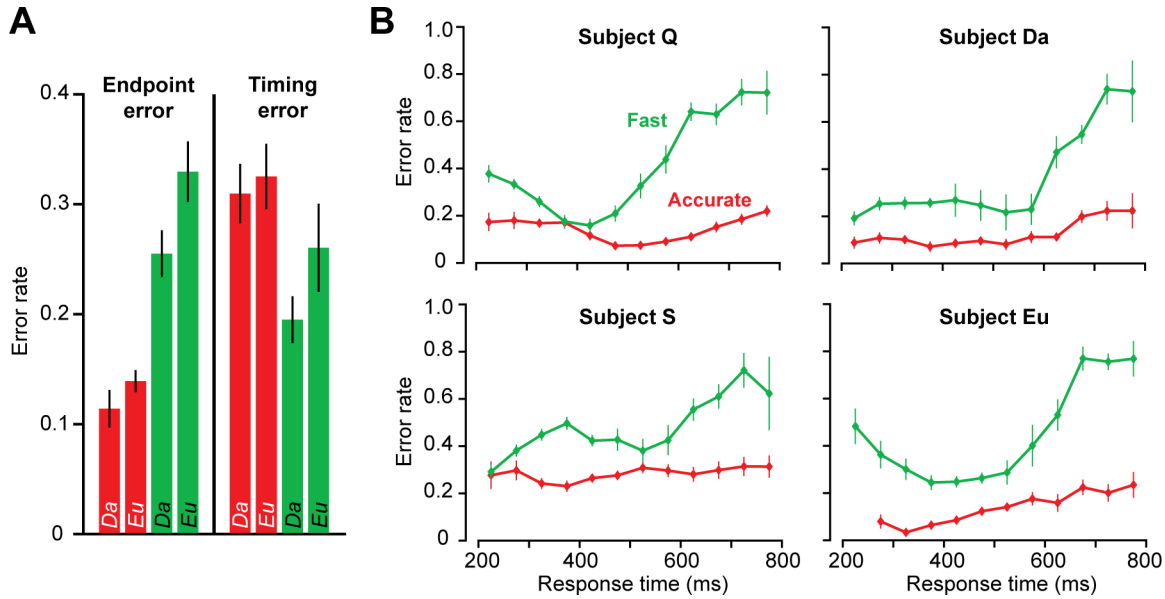

Fig. 3. Saccade end-point and timing errors. *A*: average error rates in Fast and Accurate conditions for monkeys Da and Eu. In the Fast condition, the monkeys committed more end-point errors. Conversely, in the Accurate condition, the monkeys committed more timing errors. Monkey Da generally committed fewer errors than monkey Eu. *B*: change in end-point error rate with RT. We binned end-point error rate by condition and RT and then averaged binned end-point error rate across all sessions for each monkey. Error rate increased by ~50% during the Fast condition. Error bars show means ± SE.

error rates across sessions in the Fast condition were 26% (Da; Fig. 3*A*) and 33% (Eu), whereas those in the Accurate condition were 11% (Da) and 14% (Eu). These error rates were comparable to those observed previously with monkeys Q and S. Late responses were observed in 22% (Q), 17% (S), 20% (Da), and 26% (Eu) of trials in the Fast condition. Premature responses were observed in 22% (Q), 23% (*S*), 31% (Da), and 32% (Eu) of trials in the Accurate condition.

As the monkeys adjusted RT to accommodate timing criteria in Fast and Accurate conditions, saccade error rates changed accordingly. We used RT bins of 100 ms for this analysis. We found that end-point error rate increased during the Fast condition (Fig. 3*B*; RM-ANOVA, Q: $F_{5,105} = 31.0$, $P = 6 \times 10^{-19}$; S: $F_{5,75} = 9.7$, $P = 3 \times 10^{-7}$; Da: $F_{5,40} = 23.3$, $P = 7 \times 10^{-11}$; Eu: $F_{5,30} = 21.2$, $P = 5 \times 10^{-9}$). We also found a significant change in end-point error rate during the Accurate condition (Q: $F_{5,105} = 8.0$, $P = 2 \times 10^{-6}$; S: $F_{5,80} = 2.5$, $P = 0.04$; Da: $F_{5,40} = 7.3$, $P = 6 \times 10^{-5}$; Eu: $F_{5,30} = 15.7$, $P = 1 \times 10^{-7}$). The average increase in the error rate during the Accurate condition (~10%) was much less than the average increase during the Fast condition (~50%).

Saccade vigor. Heitz and Schall (2012) motivated an interpretation of the pattern of modulation in FEF across SAT conditions by the observation that saccade velocities seemed invariant across conditions, and Heitz and Schall (2013) showed such data from a single session. Here, we examine this issue with the more sensitive measure of saccade vigor (Choi et al. 2014; Reppert et al. 2015). We fitted the equation $g(x) = \alpha \cdot x$ to the saccade main sequence for each monkey across all task-relevant saccades, producing a monkey-specific mean slope α [74.03 ± 0.09 (Q), 70.28 ± 0.12 (S), 71.54 ± 0.12 (Da), and 68.71 ± 0.16 (Eu); mean ± 95% confidence interval] with high goodness of fit for each monkey: $R^2 = 0.75$ (Q), $R^2 = 0.67$ (S), $R^2 = 0.81$ (Da), and $R^2 = 0.59$ (Eu). This one-parameter model accounted for, on average, 71% of the variance in the monkeys' saccade peak velocities.

We first asked whether the velocity profile of saccades changed with RT. For each session, we split all task-relevant saccades by condition and RT quartile, and plotted the average profile for the 1st and 4th quartiles (Fig. 4*A*, Fast condition). We focused this analysis on saccades with displacement between 4.75 and 6.5°, given that most task-relevant saccades were of this magnitude. During the Fast condition, peak velocity of saccades decreased with RT for all four monkeys [Fig. 4*B*, $t_{18} = 13.2$, $P = 1 \times 10^{-10}$ (Q), $t_{16} = 7.6$, $P = 1 \times 10^{-6}$ (S), $t_5 = 2.6$, $P = 0.049$ (Da), $t_6 = 2.7$, $P = 0.038$ (Eu)]. We observed no equivalent effect of RT on peak velocity in the Accurate condition [Fig. 4, *C* and *D*, $P = 0.74$ (Q), $P = 0.14$ (S), $P = 0.19$ (Da), $P = 0.45$ (Eu)].

We assessed whether the decrease in saccade peak velocity existed for saccades of all displacements. We found a significant decrease of saccade vigor with prolonged RT in the Fast condition (Fig. 4*E*; RM-ANOVA, Q: $F_{5,95} = 16.4$, $P = 1 \times 10^{-11}$; S: $F_{5,55} = 6.2$, $P = 1 \times 10^{-4}$; Da: $F_{5,25} = 3.5$, $P = 0.02$; Eu: $F_{5,25} = 6.7$, $P = 4 \times 10^{-4}$). Vigor decreased with RT in the Fast condition on the order of ~10% (Q), 10% (S), 15% (Da), and 15% (Eu). On average, saccade vigor decreased ~12.5% from early to late RT during the Fast condition. We found no such effect of RT on vigor for the Accurate condition.

Saccade end-point error. Given response deadlines enforced in the Fast and Accurate conditions, the probability of making a response to the appropriate stimulus decreased with faster RT (Fig. 3*A*). On trials during which the monkeys made a correct response, we assessed the mean and SD of the distribution of saccade end points relative to the target location. We defined end-point error on correct trials as the Euclidean norm of the two-dimensional vector relating measured saccade end point to actual target position. For each monkey, we computed the mean and SD of end-point error for each session. Variation in mean end-point error across monkeys was clear, but significant differences in mean end-point error were found in just one of

four monkeys. For one monkey, mean end-point error was higher during the Fast condition (Fig. 5*A*; Da: $t_8 = 3.96$, $P = 0.004$, BF = 12.80), but for three monkeys, there was no difference between conditions (Eu: $t_6 = 1.47$, $P = 0.19$, BF = 0.77; Q: $t_{20} = 1.12$, $P = 0.27$, BF = 0.40; S: $t_{16} = 1.62$, $P = 0.12$, BF = 0.74). Variation in SD of end-point error across monkeys was also clear. For two monkeys, SD of end-point error was higher during the Fast condition (Fig. 5*B*; Da: $t_8 = 3.84$, $P = 0.005$, BF = 11.13; S: $t_{16} = 3.71$, $P = 0.002$, BF = 21.86); for one monkey, there was no difference between conditions (Eu: $t_6 = 0.66$, $P = 0.53$, BF = 0.42); and for one monkey, SD was higher during the Accurate condition (Q: $t_{20} = 4.86$, $P = 9.47 \times 10^{-5}$, BF = 290.08).

Given the interaction effect of task condition (Fast vs. Accurate) and RT on saccade vigor, we asked whether there was a similar effect on end-point error of saccades. For each monkey, we performed repeated-measures ANOVA, with within-subject factor RT, on mean and SD of end-point error for each condition. We used RT bins of 100 ms for this analysis. Given the difference in RT distributions between conditions (Fig. 2), we binned RT between 200 and 600 ms for the Fast condition, and 200 and 800 ms for the Accurate condition. Regarding mean end-point error, for the Accurate condition, we found a significant interaction with RT for three monkeys (Fig. 5*C*, Da: $F_{5,40} = 2.76$, $P = 0.03$; Eu: $F_{5,30} = 2.82$, $P = 0.03$; Q: $F_{5,90} = 4.45$, $P = 0.001$), and a marginal interaction for one monkey (S: $F_{5,75} = 2.17$, $P = 0.07$). For the Fast condition, we found a significant interaction for three monkeys (Da: $F_{3,18} = 3.78$, $P = 0.03$; Q: $F_{3,54} = 4.44$, $P = 0.007$; S: $F_{3,42} = 3.40$, $P = 0.03$), and no interaction for one monkey (Eu: $F_{3,18} = 0.80$, $P = 0.51$). Regarding SD of end-point error, for the Accurate condition, we found a significant interaction with RT for two monkeys (Fig. 5*D*, Eu: $F_{5,30} = 9.93$, $P = 1.12 \times 10^{-5}$; Q: $F_{5,90} = 3.10$, $P = 0.01$), and no interaction for two monkeys (Da: $F_{5,40} = 0.71$, $P = 0.62$; S: $F_{5,75} = 1.22$, $P = 0.31$). For the Fast condition, we found a significant interaction for three monkeys (Eu: $F_{3,18} = 3.11$, $P = 0.05$; Q: $F_{3,54} = 8.09$, $P = 0.0002$, S: $F_{3,42} = 3.21$, $P = 0.03$), and no interaction for one monkey (Da: $F_{3,18} = 0.35$, $P = 0.79$). Thus, under these conditions, the SAT manipulation did not have a clear and consistent influence on saccade end-point accuracy.

Introduction of neural discharge data. The monkeys mastered the fixation-cued SAT search task well enough to alter RT immediately when the SAT cue changed (Fig. 2*B*). Adjustments in behavior were accompanied by changes in firing rate so pronounced that they were visible in the spike rasters (Fig. 6, monkey Q). Importantly, these changes in firing rate were visible even during the fixation period in some FEF neurons. As the monkeys adjusted behavior to satisfy the Fast or Accurate instruction, neurons in FEF and SC demonstrated markedly different profiles of activity. The two neurons illus-

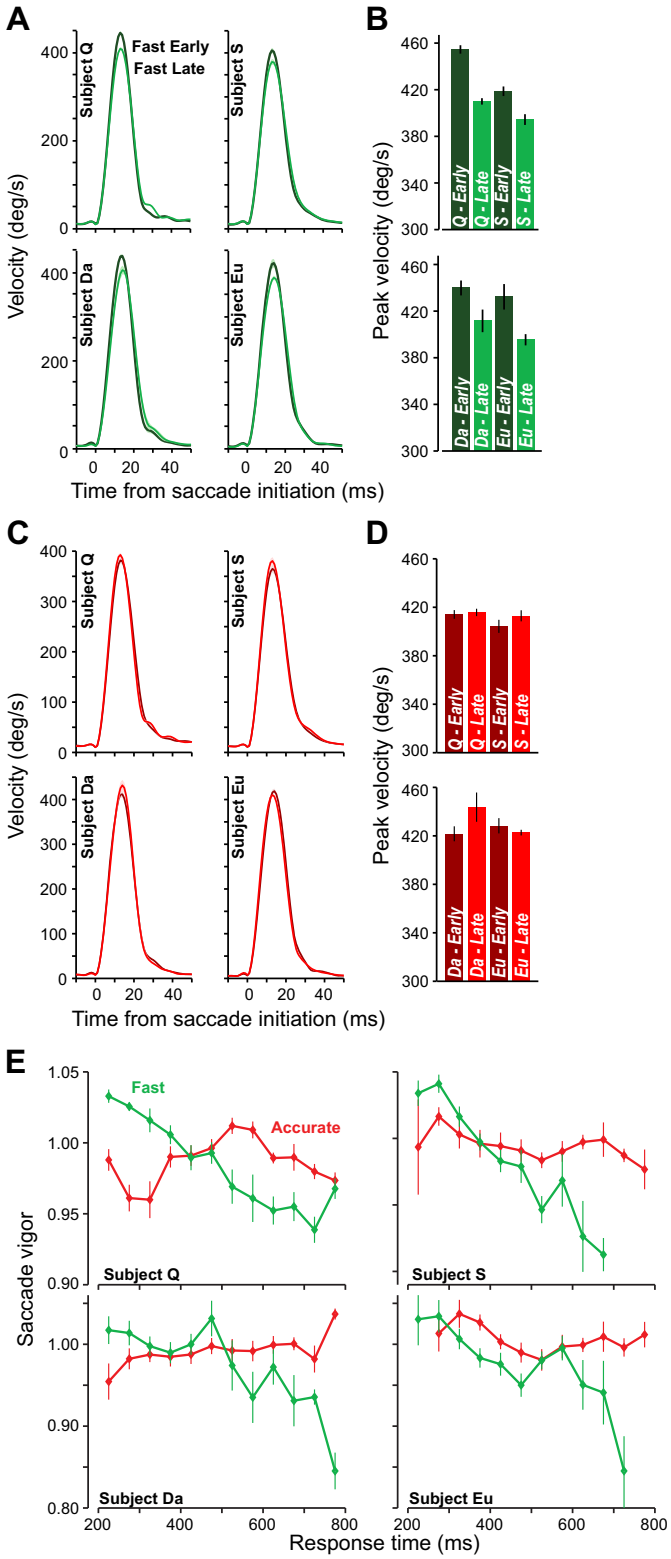

Fig. 4. Saccade vigor. *A*: average velocity profiles for early (dark green) and delayed (light green) responses in the Fast condition. For each recording session, we computed RT quartiles and average velocity profiles for the responses comprising the 1st and 4th quartiles of the RT distribution. We then averaged these profiles across recording sessions. Profiles are shown for responses with displacement between 4.75 and 6.5 deg. *B*: average peak velocity for early and late responses in the Fast condition. As in *A*, saccades belong to the 1st and 4th RT quartiles of the recording session. Peak velocity decreased with RT during the Fast condition for all four monkeys. *C*: average velocity profiles for early (dark red) and delayed (light red) responses in the Accurate condition. *D*: average peak velocity for early and late responses in the Accurate condition. *E*: change in saccade vigor with RT. We binned trials by RT and calculated the average vigor of saccades for each bin. We then averaged binned vigor across all sessions. Vigor of saccades decreased with RT in the Fast condition and varied idiosyncratically in the Accurate condition.

trated were recorded simultaneously in FEF. Parallel modulation of both neurons indicates that SAT is accomplished with a global state change influencing the networks in FEF and SC.

As in the FEF, the SAT of visual search is accomplished by multiple adjustments in the activity of distinct types of neurons in the SC. We will first describe the adjustments in baseline activity (i.e., activity before stimulus appearance) of samples of 22 visually responsive FEF neurons (Da), and 10 visually

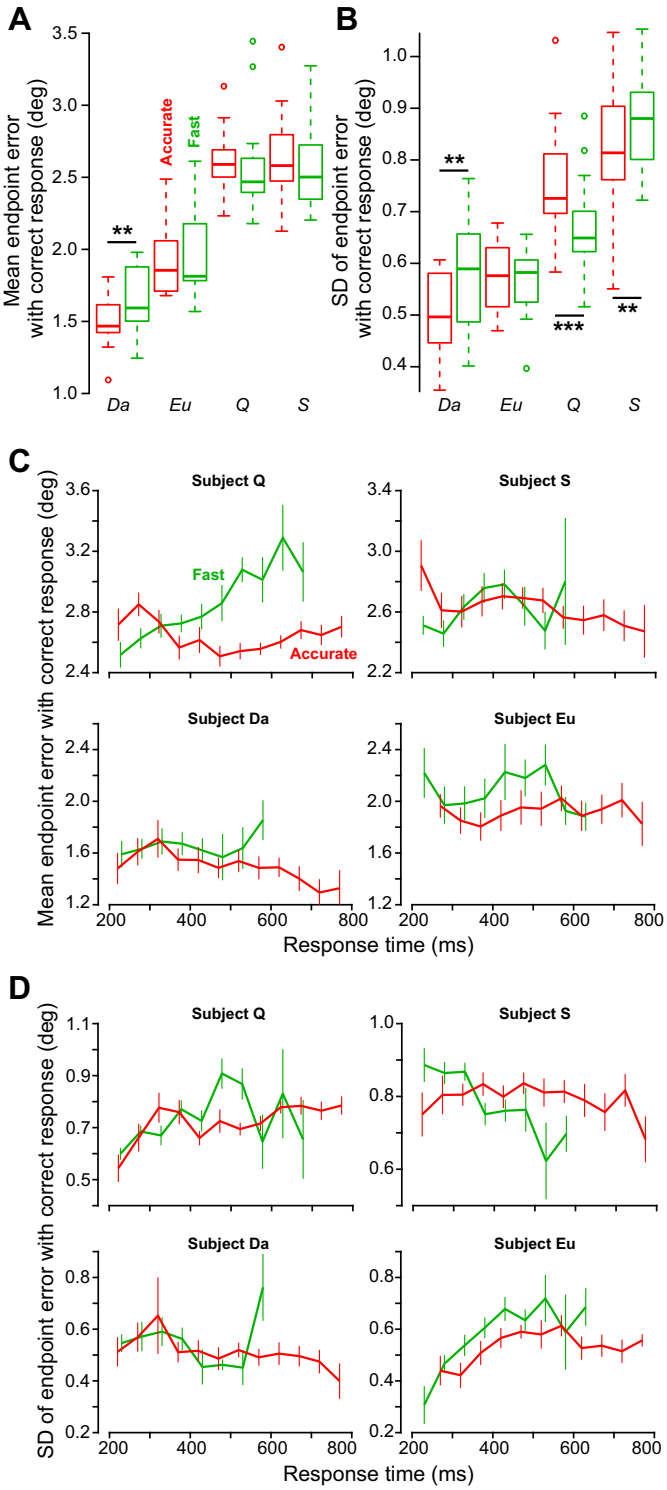

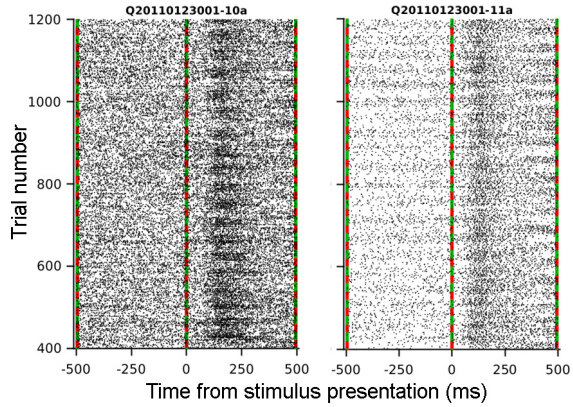

Fig. 6. Speed-accuracy modulation of discharge rates in frontal eye field (FEF). Raster plot spike times relative to array presentation for two neurons recorded simultaneously in FEF on separate electrodes during the same session. A subset of 800 trials is plotted. Trials alternated between ~20 trial blocks of Fast (green) and Accurate (red) conditions. Pronounced effects of SAT cuing were visible both before and after the array presentation.

responsive SC neurons (Da: $n = 6$; Eu: $n = 4$). These neurons increased firing rate when salient items appeared in their RF. We will assess response magnitude and TST in both sets of neurons. Visual search decisions are guided by this representation of stimulus salience in FEF (Purcell et al. 2010, 2012; Sato and Schall 2003; Sato et al. 2001; Thompson et al. 1996), posterior parietal cortex (Balan et al. 2008; Buschman and Miller 2007; Constantinidis and Steinmetz 2005; Gottlieb et al. 1998; Ipata et al. 2006; Ogawa and Komatsu 2009; Thomas and Paré 2007), substantia nigra pars reticulate (Basso and Wurtz 2002), ocular motor thalamic nuclei (Wyder et al. 2004), and SC (Kim and Basso 2008; McPeek and Keller 2002; Shen and Paré 2007; White and Munoz 2011). Data from visual and visuo-movement neurons were combined. On error trials, the visually responsive neurons exhibited increased firing rate when a distractor was placed in the neuron's RF, and a saccade was made to that distractor. We report for the first time the origin of search errors in both Fast and Accurate conditions. This analysis will include data that was previously reported (Heitz and Schall 2012) (Q: $n = 83$, S: $n = 90$; visually responsive neurons).

We will then describe saccade-related buildup activity in SC neurons (Da: $n = 2$, Eu: $n = 4$) and FEF neurons (Da: $n = 18$) that have been identified with stochastic accumulation of the salience evidence provided by visual neurons (Ratcliff et al. 2003, 2007). Pure movement neurons—those with no visual response—are encountered less commonly than neurons with

Fig. 5. Saccade end-point error relative to target position on trials with correct responses. *A*: boxplot of mean of end-point error per condition per monkey. Box hinges extend to first and third quartiles. Notches extend to $\pm 1.58 \cdot \frac{IQR}{\sqrt{n}}$ (IQR, interquartile range). Red and green boxes represent Fast and Accurate conditions, respectively. We defined end-point error as the Euclidean norm of the two-dimensional vector difference in x and y between end-point of saccade and target location. For each monkey, we computed the mean and SD of end-point error separately for each session. *B*: boxplot of SD of end-point error per condition per monkey. *C*: change in mean end-point error with RT on trials with correct responses. We binned trials by RT and calculated the mean end-point error of saccades individually for each bin. We then averaged binned end-point error across sessions. Error bars show means ± SE. *D*: change in SD of end-point error with RT. $^{**}P < 0.01$; $^{***}P < 0.001$.

Table 1. *Functional classification of neurons by structure and monkey*

	Neuron Classification			
	Visual	Visuo-Movement	Movement	Total
FEF (Q + S)	86 (55 + 31)	87 (28 + 59)	16 (7 + 9)	189 (90 + 99)
FEF (Da)	6	16	2	24
SC (Da + Eu)	5 (4 + 1)	5 (2 + 3)	1 (0 + 1)	11 (6 + 5)

Neurons from FEF were recorded from monkeys Q, S, and Da. Neurons from SC were recorded from subjects Da and Eu. Values in parentheses indicate samples from respective monkeys.

visual responses. Here, we only recorded from one pure movement-related neuron in SC, and two pure movement neurons in FEF. We will conclude with an analysis of the relationship of the activity of FEF and SC movement neurons with saccade velocity. Table 1 provides a listing of the number of neurons collected per type and monkey.

Adjustments in baseline activity. Heitz and Schall (2012) previously reported significant modulation of baseline activity in 54% of visually responsive FEF neurons. The majority of these neurons exhibited elevated activity in the Fast condition. We tested these findings in an additional set of 22 visually responsive FEF neurons (Da: Fig. 7*A*). Thirteen of 22 neurons (59%) exhibited significant modulation of activity during the baseline period (Mann-Whitney *U*-test, $P < 0.05$). Nine of these 13 neurons (69%) exhibited elevated activity in the Fast condition. However, across the population, we found no evidence for an effect of SAT condition on baseline activity in FEF (Fig. 7*C*, $t_{21} = 0.70$, $P = 0.49$, BF = 0.27). For those neurons that did exhibit a condition-cued baseline shift, what was the time course of change? We assessed trial-to-trial changes in baseline activity when there was a switch in task condition. Baseline activity of each neuron was normalized to its average firing rate during the 750 ms before array presentation. Baseline activity in FEF responded to a change in task condition within a single trial (Fig. 7*E*).

Were the effects of SAT-cued speed constraints present in SC? We next assessed baseline activity in 10 visually responsive SC cells (Da: $n = 6$; Eu: $n = 4$). The SAT cue induced a shift in baseline firing rate in visually responsive SC neurons (Fig. 7*B*). Across the population of 10 SC neurons, we found 7 neurons (3 pure visual, 4 visuo-movement) with significantly elevated activity in the Fast condition ($P < 0.05$, Mann-Whitney *U*-test). In the SC, baseline activity was significantly elevated during the Fast condition (Fig. 7*D*, $t_9 = 2.67$, $P = 0.03$, BF = 2.94). We assessed the time course of trial-to-trial changes in baseline activity in SC. Baseline activity in SC responded to a change in task condition within a single trial (Fig. 7*F*). We then compared the magnitude of SAT-related

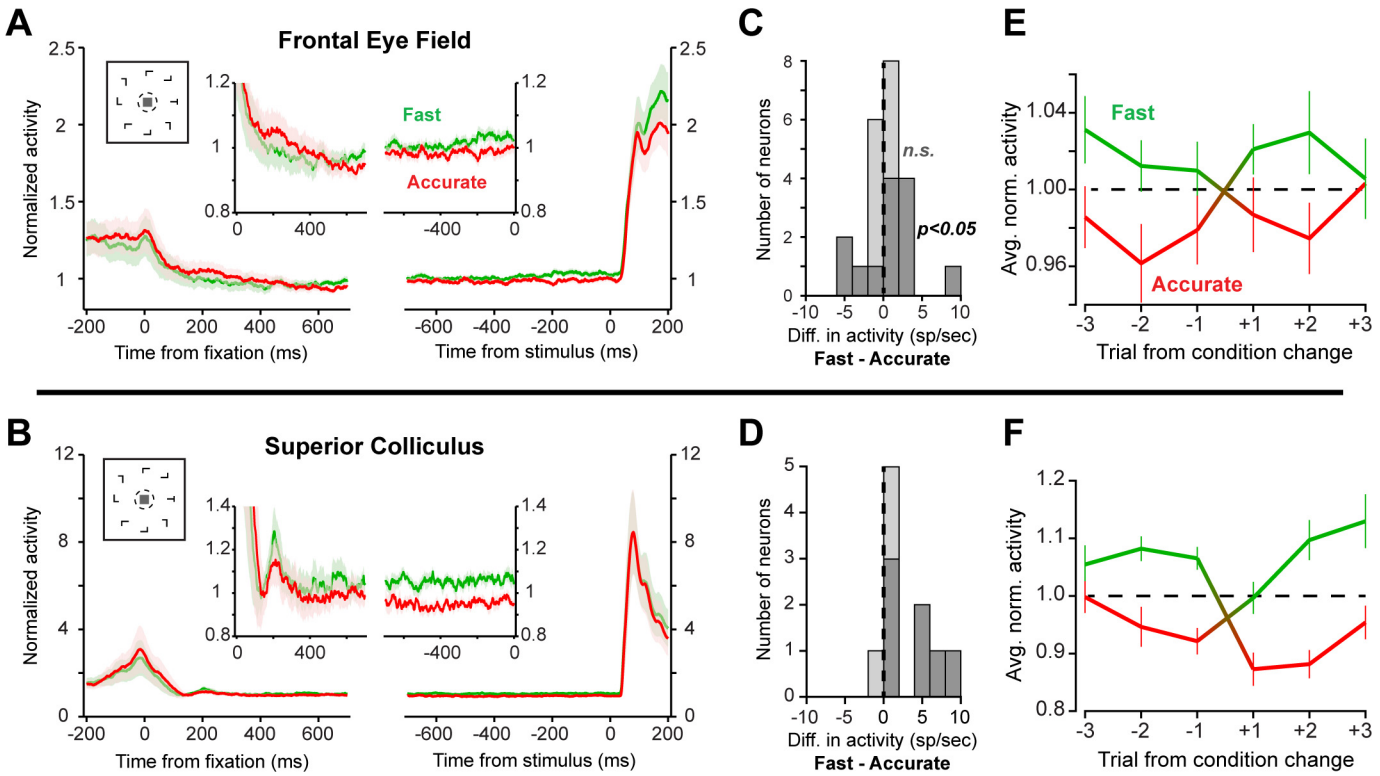

Fig. 7. Adjustment of baseline activity during speed-accuracy tradeoff. *A*: average baseline activity of 22 visually responsive frontal eye field (FEF) neurons from monkey Da. Plots on left and right are aligned on fixation of the central cue stimulus and the appearance of an array stimulus ~1 s later. Diagrammatic inset shows fixation of central cue upon the appearance of an array stimulus. Function-based inset shows baseline activity in both conditions. Baseline activity was elevated during the Fast condition. Error regions show means ± SE. *B*: average baseline activity for 10 visually responsive superior colliculus (SC) neurons. Baseline activity was elevated during the Fast condition. Conventions are the same as in *A*. *C*: histogram of difference in baseline firing rate of FEF neurons during Fast and Accurate conditions. Dark and light bars mark neurons with and without a significant change in baseline activity (Mann-Whitney *U*-test, $P < 0.05$). *D*: histogram of difference in average baseline firing rates of SC neurons. Conventions are the same as in *C*. *E*: trial-to-trial change in baseline activity of visually responsive FEF neurons at a fixation-cued change in condition. Activity of each neuron was normalized to average baseline activity across all trials, both Fast and Accurate. Error bars show means ± SE. *F*: trial-to-trial change in baseline activity of visually-responsive SC neurons at a fixation-cued change in condition. Conventions are the same as in *E*.

modulation of baseline activity in FEF and SC neurons. We found no evidence for different magnitudes of SAT-related modulation of baseline activity in FEF (0.03 ± 0.12, means ± SD) and SC (0.11 ± 0.12) ($t_{30} = 1.71$, $P = 0.10$, BF = 1.03). Neurons with and without baseline modulation were recorded within single sessions and even single electrode penetrations. Thus, SAT is accomplished, in part, through an immediate adjustment of cognitive state before stimuli are presented.

In summary, we observed elevated baseline activity in the Fast condition in SC (monkeys Da and Eu). Although some visual response FEF neurons did show elevated activity in the Fast condition, this result was not consistent across the population. Cued changes in baseline activity occurred within a single trial after a switch from Fast to Accurate or Accurate to Fast condition. The magnitude of SAT-related changes in activity was consistent across FEF and SC.

Evidence representation adjustments. Visually responsive neurons increase firing rate when salient items appear in their RF. On correct trials, all 10 visually responsive SC neurons distinguished target items from distractors by firing at a higher rate after an initial nonselective period (Fig. 8*A*; McPeek and Keller 2002; Shen and Paré 2007; White et al. 2017). We asked whether the SAT condition caused a shift in the TST between Fast and Accurate conditions. For SC neurons, the average ± SE TST in the Fast condition was 173.5 ± 13.9 ms, and that in the Accurate condition was 226.2 ± 22.6 ms. The TST was earlier in the Fast relative to the Accurate condition (Fig. 8*C*; $t_9 = 2.63$, $P = 0.03$, BF = 2.79).

Heitz and Schall (2012) previously found that in correct trials, FEF neurons selected the target among distractors earlier in the Fast relative to the Accurate condition. We replicated this finding in the new sample of FEF neurons. Seventeen of these 22 neurons (77%) distinguished target items from the distractors (Fig. 8*B*). Across this sample, for correct trials, we found evidence that TST was significantly earlier in the Fast condition (190.4 ± 8.8 ms) relative to the Accurate (206.4 ± 9.4 ms) ($t_{16} = 2.28$, $P = 0.04$, BF = 1.88) (Fig. 8*D*).

We then determined whether the SAT-related modulation in TST was different for SC and FEF. This was approached by two analyses. First, for each SC and FEF neuron that contributed to saccade target selection, we measured TST in both SAT conditions. For the analysis of FEF, we included 135 neurons from the three monkeys (Da: 17, Q: 63, S: 55). We found that, for the Accurate condition, TST in SC (226.2 ± 22.6 ms) was not significantly different from TST in FEF (247.2 ± 6.1 ms) ($t_{143} = 0.90$, $P = 0.37$, BF = 0.43); however, for the Fast condition, TST in SC (173.5 ± 13.9 ms) was marginally earlier than TST in FEF (207.1 ± 4.5 ms) $t_{143} = 1.96$, $P = 0.05$, BF = 1.44). Second, for each SC and FEF neuron, we computed the difference in TST between Fast and Accurate conditions. The average increase in TST in the Accurate relative to the Fast condition for SC (52.7 ± 20.1 ms) was not different from that for FEF (40.1 ± 5.3 ms) ($t_{143} = 0.62$, $P = 0.54$,

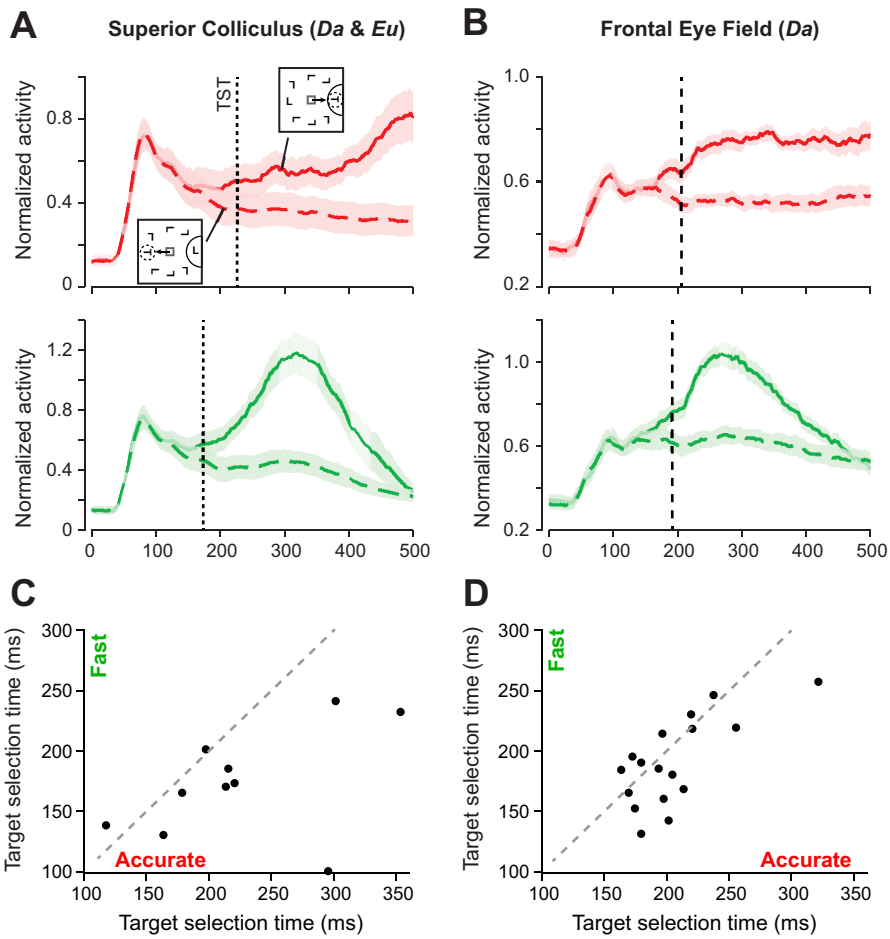

Fig. 8. Effects of speed-accuracy trade-off on salience evidence. *A*: average normalized spike density function (SDF) of visually responsive superior colliculus (SC) neurons (monkey Da: $n = 6$, monkey Eu: $n = 4$) during the 500-ms interval following presentation of the array stimulus. Density functions for Accurate (*top*) and Fast (*bottom*) conditions are shown separately. Solid and dashed lines refer to trials when the saccade was generated correctly into (solid red/green lines) or outside of (dashed red/green lines) the neuron's receptive field (RF), respectively. In both cases, we normalized each neuron's activity to maximum average firing rate during the 1-s interval after array presentation. Data from trials with correctly placed and correctly timed responses were included. Data from error trials were not included. Dashed black lines show average target selection time (TST) (173.5 ms and 226.2 ms on Fast and Accurate trials, respectively). Error regions show means ± SE. *B*: average normalized SDF of all visually responsive frontal eye field (FEF) neurons that selected the target among distractors (Da: $n = 17$). *Diagrammatic inset*: schematic of the search array on trials when the target was placed inside (*top*) and outside (*bottom*) of the neuron's RF. Average TST was 190.4 ms and 206.4 ms on Fast and Accurate trials, respectively. *C*: neuron-wise relationship between TST in the Fast and Accurate conditions for SC. Each dot represents a single neuron. Dashed line is unity. Most SC neurons had earlier TST in the Fast condition. *D*: neuron-wise relationship between TST in Fast and Accurate conditions for FEF. Most FEF neurons had earlier TST in the Fast condition.

BF = 0.37). Thus, the influence of SAT demands on the timing of target selection in SC and FEF seems equivalent or at least difficult to distinguish.

We also asked whether SAT condition affected the magnitude of the visual response in SC or FEF. For trials in each condition, we computed the maximum value of the visual response during the 150-ms interval poststimulus appearance, from which we subtracted average baseline activity. In the SC, response magnitude did not differ between Fast (120.3 sp/s) and Accurate (116.7 sp/s) conditions ($t_9 = 0.50$, $P = 0.63$, BF = 0.34). Notably, in the new sample of FEF neurons, response magnitude did not differ between Fast (31.7 sp/s) and Accurate (27.9 sp/s) conditions (Da: $t_{21} = 1.67$, $P = 0.11$, BF = 0.74).

We now describe the patterns of modulation on error trials when monkeys shifted gaze to a distractor. Heitz and Schall (2012) did not report the activity of the visually responsive target selection neurons on error trials. Obviously, more end-point error trials were collected in the Fast condition than in the Accurate condition. Hence, for the Accurate condition, for many neurons, too few error trials were observed to allow analysis. Therefore, we report population averages. In both FEF and SC, end-point errors occurred when target selection neurons treated a distractor as if it were the target. We determined whether the SAT condition affected the process of erroneous distractor selection by measuring the time course of activation of target-selection neurons in FEF and SC when *1*) the target was located in the neuron's RF, but the saccade was directed to a distractor and *2*) a distractor was located in the neuron's RF and the saccade was directed to the target outside the neuron's RF. The following analyses were completed for 143 neurons from Da (15), Q (64), and S (64) with target selection on both correct and error trials.

For each set of neurons, we computed the average normalized SDF for end-point error trials with response directed either into or outside of the neuron's movement field (Fig. 9*A*; Q, S, and Da). We estimated the average saccade-in vs. saccade-out activity for each neuron, and then applied the Mann-Whitney *U*-test to the set of average SDFs. Target selection time for FEF neurons on end-point error trials in the Fast condition was 182 ms (Q), 230 ms (S), and 226 ms (Da); average TST in the Accurate condition was 411 ms (Q), 437 ms (S), and 511 ms

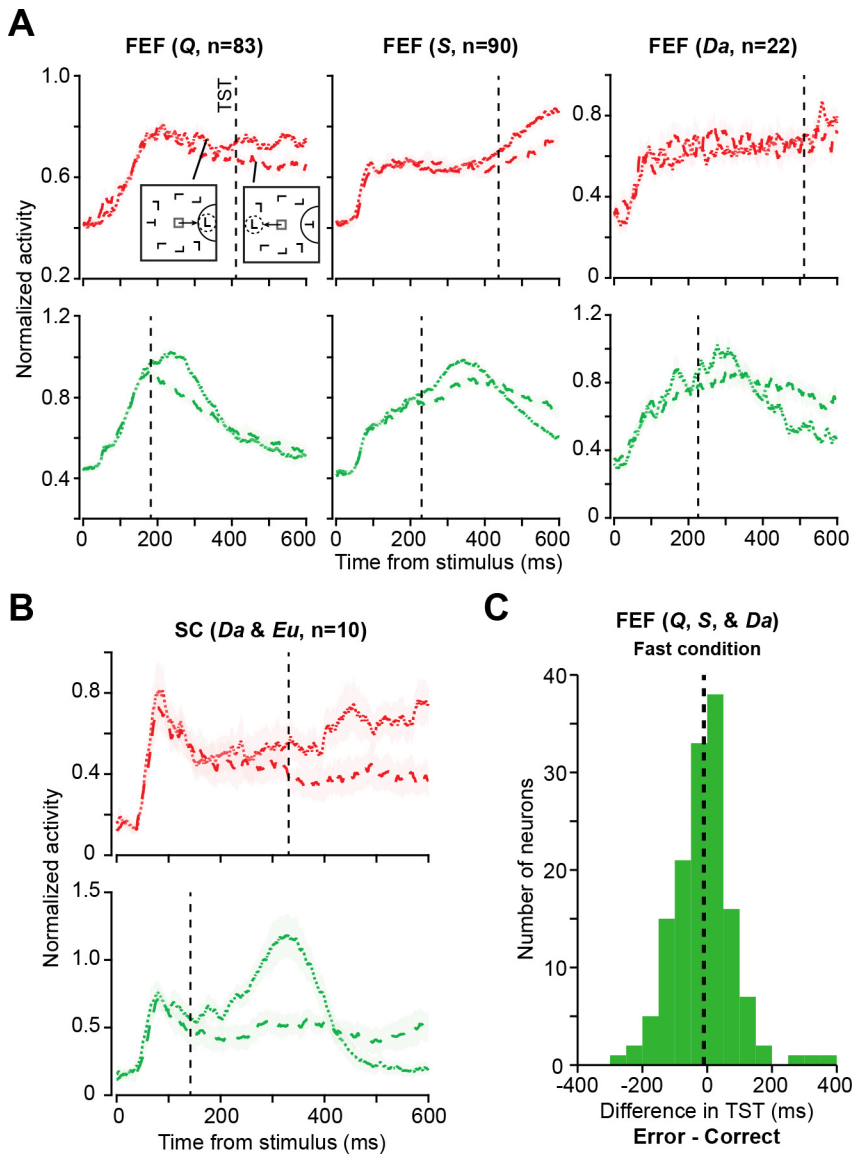

Fig. 9. Origin of targeting errors in frontal eye field (FEF) neural activity. *A*: average ± SE normalized spike density function (SDF) of all visually responsive FEF neurons (Q: $n = 83$, S: $n = 90$, and Da: $n = 22$) during the 600-ms interval following presentation of the array stimulus for Accurate (*top*) and Fast (*bottom*) conditions for trials when an errant saccade was directed to a distractor in the receptive field (RF) (dotted) and for trials when the target was in the RF but an errant saccade was directed to a distractor outside the RF (dashed). *Inset diagrams*: search array configuration and saccade direction for each trial type. Average target selection time (TST) in FEF during the Fast condition was 182 ms (Q), 230 ms (S), and 226 ms (Da); average TST in the Accurate condition was 411 ms (Q), 437 ms (S), and 511 ms (Da). *B*: average ± SE normalized SDF of all visually responsive SC neurons (Da: $n = 4$, Eu: $n = 6$). Average TST in SC was 142 ms in the Fast condition, and 331 ms in the Accurate condition. *C*: distribution of the differences between TST on trials with correct and misdirected responses. Dashed line shows across-neuron average difference of −10.3 ms. Distribution includes neurons from monkeys Q, S, and Da. The difference measure could only be computed for neurons that exhibited target selection on both correct and error trials ($n = 143$).

(Da). Average TST on error trials in SC (Fig. 9*B*; Da and Eu) was 142 ms (Fast) and 331 ms (Accurate).

We compared the time course of selection on correct and error trials. We focused this analysis on the Fast condition because end-point errors in the Accurate condition were too rare to provide a reliable estimate of TST for most neurons. Figure 9*C* shows the distribution of differences in TST between correct and error trials for all such FEF neurons. In FEF, TST was similar on error (202.6 ± 8.1 ms) and correct trials (206.1 ± 5.0 ms) ($t_{142} = 1.33$, $P = 0.19$, BF = 0.22). In SC, TST was somewhat earlier on error (134.4 ± 7.9 ms) than on correct trials (173.5 ± 13.9 ms, $t_9 = 2.33$, $P = 0.045$, BF = 1.92). The magnitude of the difference in TST between error and correct trials was indistinguishable across SC (39.1 ± 16.8 ms) and FEF (10.3 ± 7.7 ms) ($t_{151} = 0.98$, $P = 0.33$, BF = 0.46).

Response preparation adjustments. The activity of movement neurons in FEF and SC initiates saccades when a stochastic accumulation of discharge rate reaches a level that is invariant across RT (Boucher et al. 2007; Ding and Gold 2012; Hanes and Schall 1996; Pouget et al. 2011; Purcell et al. 2010, 2012; Ratcliff et al. 2007; Woodman et al. 2008). Previously, Heitz and Schall (2012) reported that presaccadic movement neurons in the FEF showed significantly greater activity on Fast relative to Accurate trials. With new data from the FEF in a third monkey and with new data from the SC in two monkeys, we determined whether this observation would be replicated (Fig. 10). We analyzed 18 FEF neurons with saccade-related buildup activity (Da: 16 visuo-movement and 2 pure movement). We normalized buildup activity to the maximum average firing rate during the peri-saccadic time interval ± 100 ms relative to saccade initiation. Across the sample, activity at saccade initiation was higher in the Fast relative to the Accurate condition. ($t_{17} = 2.38$, $P = 0.03$, BF = 2.22), replicating the previous finding (Heitz and Schall 2012). However, curiously, the build-up activity of the two pure movement neurons reached a higher value in the Accurate relative to the Fast condition (Fig. 10*B*).

We also analyzed activity from six SC neurons with presaccadic build-up activity (Da: two visuo-movement; Eu: three visuo-movement, and one pure movement) (Fig. 10*D*). In this sample of SC neurons, we found no evidence that the firing rate at saccade initiation varied across SAT conditions (Fig. 10*E*,

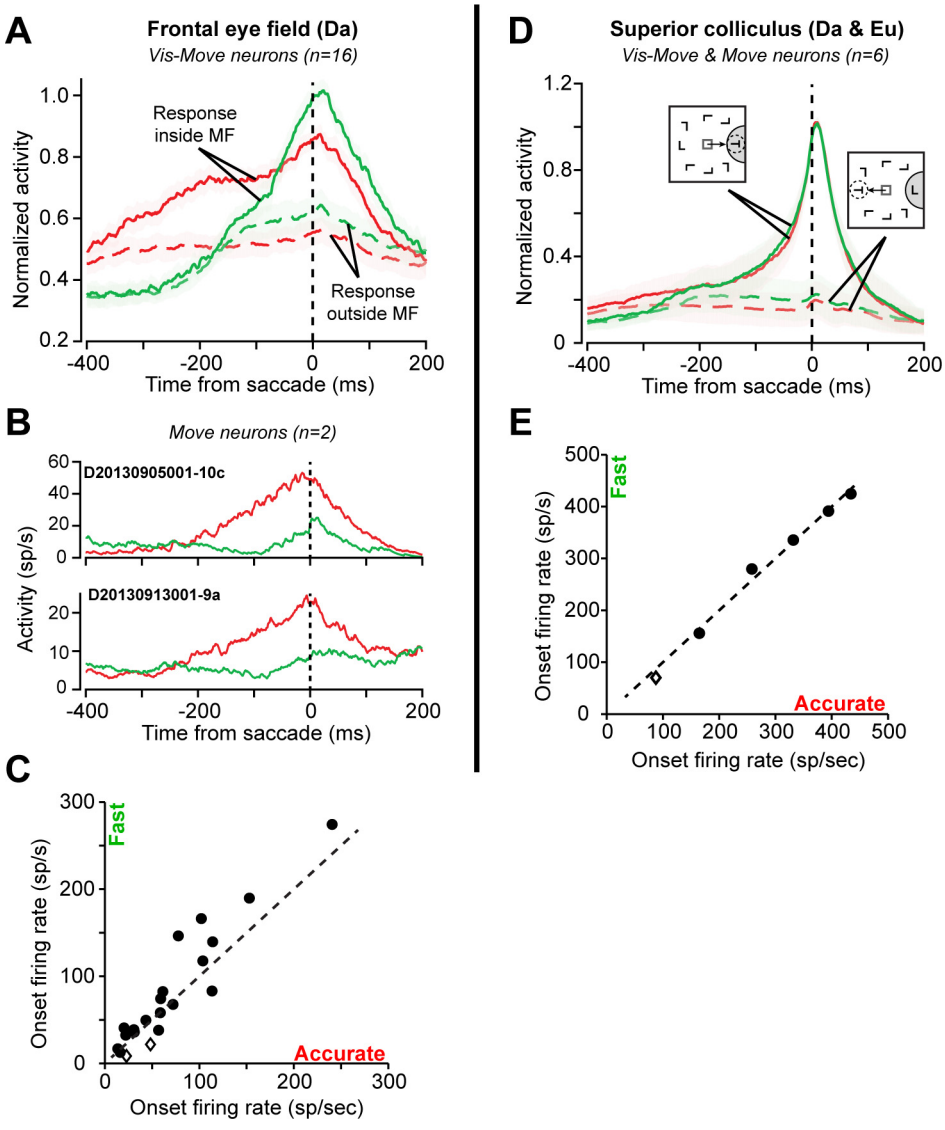

Fig. 10. Saccade-related build-up activity of frontal eye field (FEF) and superior colliculus (SC) neurons during speed-accuracy tradeoff. *A*: average normalized spike density function (SDF) of perisaccadic build-up activity across all FEF visuo-movement neurons (Da: $n = 16$). Solid and dashed lines denote trials with response directed into and outside of the neuron's MF, respectively. Build-up activity of each neuron was normalized to peak saccade-locked activity (averaged across all trials) during the interval from −100 ms to 100 ms relative to saccade. Activity of visuo-movement FEF neurons at saccade initiation was higher in the Fast condition. *B*: average SDFs of perisaccadic buildup activity of the two FEF neurons with pure movement-related activity. Activity of the two neurons at saccade initiation was higher in the Accurate condition. *C*: FEF neuron-wise relationship between activity at saccade onset in the Fast and Accurate conditions. Each dot represents a single neuron. Dashed line is unity. The two diamonds represent the pure movement neurons. Activity at saccade onset was consistently higher in the Fast condition (paired *t*-test; $P = 0.03$). *D*: average normalized SDF of perisaccadic buildup activity of all SC neurons with saccade-related activity (Da: $n = 2$, Eu: $n = 4$). Diagrammatic insets show schematic of the search array on trials with response directed into and outside of the neuron's MF. Conventions are the same as in *A*. *E*: SC neuron-wise relationship between activity at saccade onset in the Fast and Accurate conditions. Activity of movement-related SC neurons at saccade initiation was invariant across conditions (paired *t*-test, $P = 0.80$).

$t_5 = 0.27$, $P = 0.80$, BF = 0.38). Thus, SAT conditions influence presaccadic activity in FEF, but not in the SC.

Saccadic activity and saccade velocity. Presaccadic activity in the SC may have been unaffected by SAT conditions because the structure is widely acknowledged to be anatomically and functionally more directly associated with saccade generation, while FEF is less so. Given the variation of saccade velocity that we observed, we asked whether buildup activity in SC or FEF was related to peak saccade velocity. For each trial, we computed the correlation between saccade peak velocity and the average value of the single-trial SDF during the 30-ms interval after saccade initiation. We chose this interval because most task-relevant saccades had a duration of ~30 ms. In four of the six SC neurons with saccade-related activity, we observed a positive correlation between peak velocity and average firing rate (Pearson correlation coefficient: Fast condition four/six cells, $P < 0.05$; Accurate condition two/six cells, $P < 0.05$). Figure 11 shows this relationship for a neuron with a significant correlation in both conditions (Accurate: $R = 0.39$, $P = 9 \times 10^{-10}$, BF = 68.04; Fast: $R = 0.27$, $P = 0.001$, BF = 1.26). In only 4 of 18 FEF neurons with saccade-related buildup activity, we observed a positive correlation (Fast condition: 4/18 cells, $P < 0.05$; Accurate condition: 1/18 cells, $P < 0.05$, Pearson correlation coefficient). Thus, in this sample, activity correlates with velocity for of a higher fraction of saccade-related neurons in the SC relative to the FEF.

DISCUSSION

Although this article reports the fifth neurophysiological study of SAT (Hanks et al. 2014; Heitz and Schall 2012; Thura and Cisek 2016, 2017), it is a first in several respects. It is the first replication of an SAT task with new monkeys, demonstrating the reliability of this experimental approach and feasibility for future behavioral and neural studies. We confirm that the major performance measures are replicated across four monkeys. These performance measures include the first description of the relationship between response time and the deadlines used to enforce the SAT conditions. Also, we report how error rate varies systematically with response time within SAT conditions. These relationships, which were unknown before, invite further examination of existing data sets and provide necessary information for future models of SAT in this task.

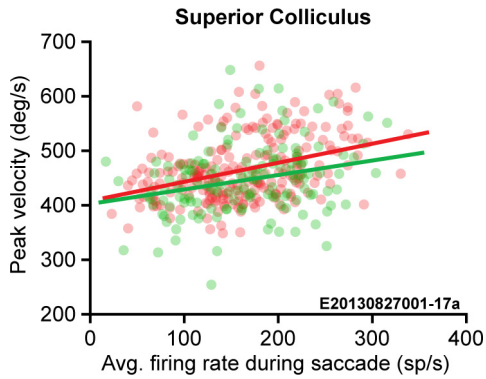

Fig. 11. Peak velocity and saccade activity in superior colliculus (SC). Relationship between saccadic peak velocity and maximum firing rate for representative SC neuron from monkey Eu. Each point represents a single trial. Red and green dots represent data from Accurate and Fast trials, respectively. Peak velocity of saccades increased with average saccade-related activity for this neuron (Accurate: $R = 0.39$, $P = 9 \times 10^{-10}$, BF = 68.04; Fast: $R = 0.27$, $P = 0.001$, BF = 1.26). We observed a positive correlation between maximum firing rate and saccadic peak velocity during at least one condition for four out of six SC neurons with saccade-related activity.

This article is the first detailed description of the variation of saccade dynamics with SAT conditions, monkeys, and response time. The idiosyncratic and systematic variation of saccade dynamics contradicts a basic assumption motivating an integrated accumulator explanation of FEF movement neuron modulation during SAT (Heitz and Schall 2012). Thus, more elaborate models are needed to understand how saccade-related discharges in the FEF and the SC relate to saccade dynamics.

This article is the first description of neural adjustments in SC with visual search SAT. Although the sample size from the SC is smaller than desirable, we believe reasonable confidence is warranted in the reliability of the results for the following reasons. First, the performance of the two additional monkeys replicated that of the original two monkeys. Second, the new sample of visual salience neurons in FEF replicated the major observations reported previously (Heitz and Schall 2012). Third, the quantitative nature of movement neuron activation at RT being higher in Accurate relative to Fast trials is theoretically very important. Fourth, the general pattern of modulation of SC neurons during visual search replicates previous observations by multiple laboratories (e.g., McPeek and Keller 2002; Shen and Paré 2007; White and Munoz 2011; White et al. 2017). Fifth, each new observation was replicated across monkeys and neurons. Thus, although a larger sample of neurons would increase statistical power, given the well-known, consistent patterns of SC modulation, it is unlikely that the results would change. In spite of the small sample size, the conclusions that we draw are supported by Bayes factors.

These new data confirm earlier neurophysiological findings, showing that SAT is accomplished by a multitude of mechanistically distinct adjustments. As in FEF, when accuracy was cued, proactive baseline discharge rate in SC was reduced. We demonstrate that this modulation occurs immediately upon SAT cue changes and becomes more efficient in successive trials. Unlike FEF, the magnitude of visual responses in SC to the search array did not vary with SAT condition. This invariance across SAT conditions makes the SC also different from LIP (Hanks et al. 2014) and premotor and motor cortex (Thura and Cisek 2016).

However, like the FEF, the target selection process in SC took more time in the Accurate compared with the Fast condition. This was so even on targeting error trials when a distractor was mistaken for a target. Indeed, we provide the first evidence that errors in SAT can arise through incorrect representation of the evidence. As observed previously (Heitz et al., 2010; Thompson et al., 2005), search errors occurred when visual target selection neurons in the FEF and SC treated a distractor as if it were the target. In the other neurophysiological studies of the SAT, it is not known how the errors arise.

The SC was different from the FEF in another theoretically important respect. The original report of FEF adjustments during SAT described higher presaccadic movement neuron activity at saccade initiation in Fast relative to Accurate SAT conditions (Heitz and Schall 2012). In SC, we found that presaccadic movement neuron activity at saccade initiation was invariant across SAT conditions. Curiously, in the sample of FEF neurons collected during the same period, the two presac-

cadic movement neurons sampled showed the opposite pattern with higher presaccadic movement neuron activity at saccade initiation in Accurate relative to Fast SAT conditions. Whether this is a sampling anomaly or a sign of individual differences cannot be resolved at this time. The invariance observed in SC but not FEF can be understood from the perspective that relative to FEF, SC is functionally closer to the saccade generation process. Indeed, we also found that during saccade production, discharge rates in SC, but less so in FEF, were correlated with saccade velocity (see also, Goosens and Van Opstal 2006).

Further insight can be gained by comparing these findings to the two other neurophysiological investigations of SAT. Thura and Cisek (2016) report data from premotor and primary motor cortex of two monkeys tested in a reaching task that encouraged Fast or Accurate responses in interleaved blocks. Premotor and motor cortex neurons exhibited early elevated discharge rates in Fast relative to Accurate trials. However, like these SC results, the discharge rate at movement initiation in the premotor and motor cortex was invariant across conditions. Hanks et al. (2014) report data from area LIP of two monkeys obtained in separate Fast and Accurate testing sessions. Distinct manipulations of task contingencies were needed to adapt each monkeys' performance. Among neurons sampled in these separate sessions, patterns of SAT modulation varied across monkeys, but a trend for higher discharge rates in the Fast relative to the Accurate condition was found. In the final 75 ms before saccade production, LIP neural activity reached invariant levels across SAT conditions. It should be noted that the presaccadic activity in LIP does not have the same anatomical or causal relation to movement initiation as that measured in movement neurons in FEF, SC, premotor, or motor cortex. To summarize, across all of these data sets from different brain structures sampled in different laboratories and testing conditions, the modulation of the early activity, being higher for Fast relative to Accurate trials, is a robust finding. Also, across the four data sets, invariance of premovement activity across SAT conditions was the most common finding.

Taken together, these results verify basic elements of previous observations and, thus, advance our understanding of the neural mechanisms of SAT. The general theoretical implications of these SAT neurophysiology data have been detailed before (Heitz and Schall, 2012, 2013). The specific implications of these new observations will be worked out through formal computational models of how salience evidence can be accumulated to guide gaze (Purcell et al., 2010, 2012) (M. Servant, unpublished data). Overall, the neurophysiological investigation of SAT is revealing unexpected, important, and useful new insights.

ACKNOWLEDGMENTS

We thank J. Easley, M. Feurtado, M. Maddox, S. Motorny, J. Parker, M. Schall, and L. Toy for animal care and other technical assistance.

GRANTS

This research was funded by National Eye Institute Grants F32-EY019851 (R. P. Heitz), T32-EY007135 (T. R. Reppert), R01-EY08890 (J. D. Schall), P30-EY08126 (T. R. Reppert, M. Servant, R. P. Heitz, J. D. Schall) and by National Institute of Child Health and Human Development Grant U54-HD083211 (T. R. Reppert, M. Servant, R. P. Heitz, J. D. Schall). Additional support was provided by Robin and Richard Patton through the E. Bronson Ingram Chair in Neuroscience.

DISCLOSURES

No conflicts of interest, financial or otherwise, are declared by the authors.

AUTHOR CONTRIBUTIONS

T.R.R., M.S., and R.P.H. analyzed data; T.R.R., M.S., R.P.H., and J.D.S. interpreted results of experiments; T.R.R. and J.D.S. prepared figures; T.R.R. drafted manuscript; T.R.R., M.S., R.P.H., and J.D.S. edited and revised manuscript; T.R.R., M.S., R.P.H., and J.D.S. approved final version of manuscript; R.P.H. and J.D.S. conceived and designed research; R.P.H. performed experiments.

REFERENCES

Bahill AT, Clark MR, Stark L. The main sequence, a tool for studying human eye movements. *Math Biosci* 24: 191–204, 1975. doi:10.1016/0025-5564(75)90075-9.

Balan PF, Oristaglio J, Schneider DM, Gottlieb J. Neuronal correlates of the set-size effect in monkey lateral intraparietal area. *PLoS Biol* 6: e158, 2008. doi:10.1371/journal.pbio.0060158.

Basso MA, Wurtz RH. Neuronal activity in substantia nigra pars reticulata during target selection. *J Neurosci* 22: 1883–1894, 2002. doi:10.1523/JNEUROSCI.22-05-01883.2002.

Boucher L, Palmeri TJ, Logan GD, Schall JD. Inhibitory control in mind and brain: an interactive race model of countermanding saccades. *Psychol Rev* 114: 376–397, 2007. doi:10.1037/0033-295X.114.2.376.

Buschman TJ, Miller EK. Top-down versus bottom-up control of attention in the prefrontal and posterior parietal cortices. *Science* 315: 1860–1862, 2007. doi:10.1126/science.1138071.

Choi JES, Vaswani PA, Shadmehr R. Vigor of movements and the cost of time in decision making. *J Neurosci* 34: 1212–1223, 2014. doi:10.1523/JNEUROSCI.2798-13.2014.

Cohen JY, Pouget P, Heitz RP, Woodman GF, Schall JD. Biophysical support for functionally distinct cell types in the frontal eye field. *J Neurophysiol* 101: 912–916, 2009. doi:10.1152/jn.90272.2008.

Collewijn H, Erkelens CJ, Steinman RM. Binocular co-ordination of human horizontal saccadic eye movements. *J Physiol* 404: 157–182, 1988. doi:10.1113/jphysiol.1988.sp017284.

Constantinidis C, Steinmetz MA. Posterior parietal cortex automatically encodes the location of salient stimuli. *J Neurosci* 25: 233–238, 2005. doi:10.1523/JNEUROSCI.3379-04.2005.

Ding L, Gold JI. Caudate encodes multiple computations for perceptual decisions. *J Neurosci* 30: 15747–15759, 2010. doi:10.1523/JNEUROSCI.2894-10.2010.

Ding L, Gold JI. Neural correlates of perceptual decision making before, during, and after decision commitment in monkey frontal eye field. *Cereb Cortex* 22: 1052–1067, 2012. doi:10.1093/cercor/bhr178.

Goosens HH, van Opstal AJ. Dynamic ensemble coding of saccades in the monkey superior colliculus. *J Neurophysiol* 95: 2326–2341, 2006. doi:10.1152/jn.00889.2005.

Gottlieb JP, Kusunoki M, Goldberg ME. The representation of visual salience in monkey parietal cortex. *Nature* 391: 481–484, 1998. doi:10.1038/35135.

Gregoriou GG, Gotts SJ, Desimone R. Cell-type-specific synchronization of neural activity in FEF with V4 during attention. *Neuron* 73: 581–594, 2012. doi:10.1016/j.neuron.2011.12.019.

Hanes DP, Schall JD. Neural control of voluntary movement initiation. *Science* 274: 427–430, 1996. doi:10.1126/science.274.5286.427.

Hanks T, Kiani R, Shadlen MN. A neural mechanism of speed-accuracy tradeoff in macaque area LIP. *eLife* 3: e02260, 2014. doi:10.7554/eLife.02260.

Heitz RP. The speed-accuracy tradeoff: history, physiology, methodology, and behavior. *Front Neurosci* 8: 150, 2014. doi:10.3389/fnins.2014.00150.

Heitz RP, Cohen JY, Woodman GF, Schall JD. Neural correlates of correct and errant attentional selection revealed through N2pc and frontal eye field activity. *J Neurophysiol* 104: 2433–2441, 2010. doi:10.1152/jn.00604.2010.

Heitz RP, Engle RW. Focusing the spotlight: individual differences in visual attention control. *J Exp Psychol Gen* 136: 217–240, 2007. doi:10.1037/0096-3445.136.2.217.

Heitz RP, Schall JD. Neural mechanisms of speed-accuracy tradeoff. *Neuron* 76: 616–628, 2012. doi:10.1016/j.neuron.2012.08.030.

Heitz RP, Schall JD. Neural chronometry and coherency across speed-accuracy demands reveal lack of homomorphism between computational and neural mechanisms of evidence accumulation. *Philos Trans R Soc Lond B Biol Sci* 368: 20130071, 2013. doi:10.1098/rstb.2013.0071.

Ipata AE, Gee AL, Goldberg ME, Bisley JW. Activity in the lateral intraparietal area predicts the goal and latency of saccades in a free-viewing visual search task. *J Neurosci* 26: 3656–3661, 2006. doi:10.1523/JNEUROSCI.5074-05.2006.

Kim B, Basso MA. Saccade target selection in the superior colliculus: a signal detection theory approach. *J Neurosci* 28: 2991–3007, 2008. doi:10.1523/JNEUROSCI.5424-07.2008.

Kim J-N, Shadlen MN. Neural correlates of a decision in the dorsolateral prefrontal cortex of the macaque. *Nat Neurosci* 2: 176–185, 1999. doi:10.1038/5739.

Latimer KW, Yates JL, Meister MLR, Huk AC, Pillow JW. Single-trial spike trains in parietal cortex reveal discrete steps during decision-making. *Science* 349: 184–187, 2015. doi:10.1126/science.aaa4056.

McPeek RM, Keller EL. Saccade target selection in the superior colliculus during a visual search task. *J Neurophysiol* 88: 2019–2034, 2002. doi:10.1152/jn.2002.88.4.2019.

Ogawa T, Komatsu H. Condition-dependent and condition-independent target selection in the macaque posterior parietal cortex. *J Neurophysiol* 101: 721–736, 2009. doi:10.1152/jn.90817.2008.

Pouget P, Logan GD, Palmeri TJ, Boucher L, Paré M, Schall JD. Neural basis of adaptive response time adjustment during saccade countermanding. *J Neurosci* 31: 12604–12612, 2011. doi:10.1523/JNEUROSCI.1868-11.2011.

Purcell BA, Heitz RP, Cohen JY, Schall JD, Logan GD, Palmeri TJ. Neurally constrained modeling of perceptual decision making. *Psychol Rev* 117: 1113–1143, 2010. doi:10.1037/a0020311.

Purcell BA, Schall JD, Logan GD, Palmeri TJ. From salience to saccades: multiple-alternative gated stochastic accumulator model of visual search. *J Neurosci* 32: 3433–3446, 2012. doi:10.1523/JNEUROSCI.4622-11.2012.

Ratcliff R, Cherian A, Segraves M. A comparison of macaque behavior and superior colliculus neuronal activity to predictions from models of two-choice decisions. *J Neurophysiol* 90: 1392–1407, 2003. doi:10.1152/jn.01049.2002.

Ratcliff R, Hasegawa YT, Hasegawa RP, Smith PL, Segraves MA. Dual diffusion model for single-cell recording data from the superior colliculus in a brightness-discrimination task. *J Neurophysiol* 97: 1756–1774, 2007. doi:10.1152/jn.00393.2006.

Ray S, Pouget P, Schall JD. Functional distinction between visuomovement and movement neurons in macaque frontal eye field during saccade countermanding. *J Neurophysiol* 102: 3091–3100, 2009. doi:10.1152/jn.00270.2009.

Reppert TR, Lempert KM, Glimcher PW, Shadmehr R. Modulation of saccade vigor during value-based decision making. *J Neurosci* 35: 15369–15378, 2015. doi:10.1523/JNEUROSCI.2621-15.2015.

Rinkenauer G, Osman A, Ulrich R, Muller-Gethmann H, Mattes S. On the locus of speed-accuracy trade-off in reaction time: inferences from the lateralized readiness potential. *J Exp Psychol Gen* 133: 261–282, 2004. doi:10.1037/0096-3445.133.2.261.

Roitman JD, Shadlen MN. Response of neurons in the lateral intraparietal area during a combined visual discrimination reaction time task. *J Neurosci* 22: 9475–9489, 2002. doi:10.1523/JNEUROSCI.22-21-09475.2002.

Rouder JN, Morey RD, Speckman PL, Province JM. Default Bayes factors for ANOVA designs. *J Math Psychol* 56: 356–374, 2012. doi:10.1016/j.jmp.2012.08.001.

Rouder JN, Speckman PL, Sun D, Morey RD, Iverson G. Bayesian *t* tests for accepting and rejecting the null hypothesis. *Psychon Bull Rev* 16: 225–237, 2009. doi:10.3758/PBR.16.2.225.

Sato T, Murthy A, Thompson KG, Schall JD. Search efficiency but not response interference affects visual selection in frontal eye field. *Neuron* 30: 583–591, 2001. doi:10.1016/S0896-6273(01)00304-X.

Sato TR, Schall JD. Effects of stimulus-response compatibility on neural selection in frontal eye field. *Neuron* 38: 637–648, 2003. doi:10.1016/S0896-6273(03)00237-X.

Shen K, Paré M. Neuronal activity in superior colliculus signals both stimulus identity and saccade goals during visual conjunction search. *J Vis* 7: 15.1–15.13, 2007. doi:10.1167/7.5.15.

Thomas NWD, Paré M. Temporal processing of saccade targets in parietal cortex area LIP during visual search. *J Neurophysiol* 97: 942–947, 2007. doi:10.1152/jn.00413.2006.

Thompson KG, Bichot NP, Sato TR. Frontal eye field activity before visual search errors reveals the integration of bottom-up and top-down salience. *J Neurophysiol* 93: 337–351, 2005. doi:10.1152/jn.00330.2004.

Thompson KG, Hanes DP, Bichot NP, Schall JD. Perceptual and motor processing stages identified in the activity of macaque frontal eye field neurons during visual search. *J Neurophysiol* 76: 4040–4055, 1996. doi:10.1152/jn.1996.76.6.4040.

Thura D, Beauregard-Racine J, Fradet C-W, Cisek P. Decision making by urgency gating: theory and experimental support. *J Neurophysiol* 108: 2912–2930, 2012. doi:10.1152/jn.01071.2011.

Thura D, Cisek P. Modulation of premotor and primary motor cortical activity during volitional adjustments of speed-accuracy trade-offs. *J Neurosci* 36: 938–956, 2016. doi:10.1523/JNEUROSCI.2230-15.2016.

Thura D, Cisek P. The basal ganglia do not select reach targets but control the urgency of commitment. *Neuron* 95: 1160–1170.e5, 2017. doi:10.1016/j.neuron.2017.07.039.

White BJ, Kan JY, Levy R, Itti L, Munoz DP. Superior colliculus encodes visual saliency before the primary visual cortex. *Proc Natl Acad Sci USA* 114: 9451–9456, 2017. doi:10.1073/pnas.1701003114.

White BJ, Munoz DP. Separate visual signals for saccade initiation during target selection in the primate superior colliculus. *J Neurosci* 31: 1570–1578, 2011. doi:10.1523/JNEUROSCI.5349-10.2011.

Wong K-F, Huk AC, Shadlen MN, Wang X-J. Neural circuit dynamics underlying accumulation of time-varying evidence during perceptual decision making. *Front Comput Neurosci* 1: 6, 2007. doi:10.3389/neuro.10.006.2007.

Woodman GF, Kang M-S, Thompson K, Schall JD. The effect of visual search efficiency on response preparation: neurophysiological evidence for discrete flow. *Psychol Sci* 19: 128–136, 2008. doi:10.1111/j.1467-9280.2008.02058.x.

Wyder MT, Massoglia DP, Stanford TR. Contextual modulation of central thalamic delay-period activity: representation of visual and saccadic goals. *J Neurophysiol* 91: 2628–2648, 2004. doi:10.1152/jn.01221.2003.

Yates JL, Park IM, Katz LN, Pillow JW, Huk AC. Functional dissection of signal and noise in MT and LIP during decision-making. *Nat Neurosci* 20: 1285–1292, 2017. doi:10.1038/nn.4611.